The Kuroshio Extension and its recirculation gyres

Steven R. Jayne[1], Nelson G. Hogg[2], Stephanie N. Waterman[3], Luc Rainville[4], Kathleen A. Donohue[5], D. Randolph Watts[5], Karen L. Tracey[5] Julie L. McClean[6], Mathew E. Maltrud[7], Bo Qiu[8], Shuiming Chen[8], and Peter Hacker[8]

Abstract.
This paper reports on the strength and structure of the Kuroshio Extension and its recirculation gyres. In the time average, quasi-permanent recirculation gyres are found to the north and south of the Kuroshio Extension jet. The characteristics of recirculation gyres are determined from the combined observations from the Kuroshio Extension System Study (KESS) field program program (June 2004 – June 2006) and include current meters, pressure and current recording inverted echo sounders, and sub-surface floats. The position and strength of the recirculation gyres simulated by a high-resolution numerical model are found to be consistent with the observations.
The circulation pattern that is revealed is of a complex system of multiple recirculation gyres that are embedded in the crests and troughs of the quasi-permanent meanders of the Kuroshio Extension. At the location of the KESS array, the Kuroshio Extension jet and its recirculation gyres transport of about 114 Sv. This represents a 2.7-fold increase in the transport of the current compared to the Kuroshio's transport at Cape Ashizuri before it separates from the coast and flows eastward into the open ocean. This enhancement in the current's transport comes from the development of the flanking recirculation gyres. Estimates from an array of inverted echo sounders and a high-resolution ocean general circulation model are of similar magnitude.

1. Introduction

The warm, northward-flowing waters of the Kuroshio separate from the Japanese coast at the Bōsō Peninsula to flow eastward into the North Pacific Ocean as a free jet – the Kuroshio Extension (see Kawai 1972; Mizuno and White 1983; Qiu 2002; Yasuda 2003, for an overview of the Kuroshio Extension system). Separated western boundary currents, such as the Kuroshio Extension and the Gulf Stream often have associated recirculation gyres (Hogg and Johns 1995). The development of flanking, weakly depth-dependent recirculation gyres significantly increases the downstream transport of the separated jet (Richardson 1985; Schmitz and McCartney 1993). By providing quasi-stable regions where water can be trapped for long periods, they are sites for deep wintertime convection, formation regions of mode waters, and reservoirs of heat and potential vorticity. Furthermore, eddy variability appears to be important in coupling the strong motions in these baroclinic jets to deep abyssal circulations, driving the deep recirculation gyres (Hogg 1983, 1985, 1993) and potentially acting back on the upper jet, influencing its speed and direction (Cronin and Watts 1996; Cronin 1996).

A variety of mechanisms have been offered for produc-

[1]Physical Oceanography Dept., Woods Hole Oceanographic Institution, Woods Hole, MA
[2]Earth and Atmospheric Sciences, Cornell University, Ithaca, NY
[3]MIT/WHOI Joint Program in Oceanography, Woods Hole Oceanographic Institution, Woods Hole, MA, now at National Oceanography Centre, Southampton, UK
[4]Applied Physics Laboratory, University of Washington, Seattle, WA
[5]Graduate School of Oceanography, University of Rhode Island, Narragansett, RI
[6]Physical Oceanography Research Division, Scripps Institution of Oceanography, La Jolla, CA
[7]Theoretical Fluid Dynamics Group, Los Alamos National Laboratory, Los Alamos, NM
[8]Department of Oceanography, University of Hawaii at Manoa, Honolulu, HI

ing the intense recirculation zones found in the vicinity of western boundary currents. A hypothesis is that they result from the need of the inertial, baroclinic western boundary current to rid itself of anomalous potential vorticity which it acquired at other latitudes, prior to separating from the coast. Three classes of theories appear in the literature to explain how this occurs. The first are inertial theories in which time-mean recirculation gyres can arise from the steady-state time-mean advection of potential vorticity alone (*e.g.* Fofonoff 1954; Marshall and Nurser 1986; Greatbatch 1987; Cessi 1990; Nakano et al. 2008). The second group are theories in which the eddy fluxes resulting from a directly prescribed vorticity forcing generate mean rectified flows through eddy-mean flow and eddy-eddy interactions (*e.g.* Haidvogel and Rhines 1983; Cessi et al. 1987; Malanotte-Rizzoli et al. 1995; Berloff 2005). Finally, the third group of theories derives from studies of unstable jets in which the generation of mean recirculations results from the combination of eddy effects (arising from jet instabilities) and inertial effects (*e.g.* Spall 1994; Jayne et al. 1996; Beliakova 1998; Jayne and Hogg 1999; Mizuta 2009). These theories and their relevance to the Kuroshio Extension are discussed in more depth by Waterman (2009).

Recirculation gyres flank the Gulf Stream after it separates from the coast of North America on both the jet's north and south sides (Worthington 1976; Richardson 1985; Hogg et al. 1986; Hogg 1992). These elongated recirculation gyres are of approximately equal strength and enhance the transport of the Gulf Stream from 31 Sv in the Florida Straits (Beal et al. 2008) to approximately 85 Sv at its separation point at Cape Hatteras to 150 Sv at 60°W (Hogg 1992). In the case of the Kuroshio Extension, the situation is less clear. A westward recirculation has been observed south of the first crest in the Kuroshio Extension in the WOCE P10 section using a lowered ADCP (Firing 1998; Wijffels et al. 1998). This southern recirculation gyre is also clear in altimetry observations of the Kuroshio Extension (Qiu et al. 1991; Qiu and Chen 2005) and in subsurface drifting float observations (Chen et al. 2007; Qiu et al. 2008). Additionally there is a surface expression of the southern recirculation gyre observed by drifters (Niiler et al. 2003b). However to the north of the current, the presence or absence of a permanent recirculation may be interrupted by smaller scale transient features and may depend on measurement depth and location. It is absent from the regional mean circulation derived from hydrography (Teague et al. 1990) and a careful compilation of deep current meter records by Owens and Warren (2001) supports neither the presence nor the absence of such a gyre. Westward deep counter currents were observed both to the south and north of the Kuroshio in two synoptic sections using lowered acoustic Doppler current profilers (ADCP) by Yoshikawa et al. (2004). However, single synoptic sections can not establish their permanence due to highly variable nature of rings and meanders in the Kuroshio Extension. On the other hand, using a compilation of profiling floats in the Kuroshio Extension, Qiu et al. (2008) infer a weak recirculation pattern north of the jet from the long-term and spatially-smoothed average of profiling float displacements at 1500 m. Furthermore, in a study using a high-resolution model, Nakano et al. (2008) found a chain of multiple recirculation gyres flanking the Kuroshio Extension in their modeling study. Of note from that work, is that while the recirculation gyres are not apparent in the surface fields, they dominate the abyssal flow field.

In this paper, we report on evidence of quasi-permanent recirculation gyres to both the south and north of the Kuroshio Extension from *in situ* observations. The observational data come from instrumentation deployed for a 2-year period during the Kuroshio Extension System Study (KESS). Measurements from moored current meters provide clear evidence for these recirculation gyres, as do observations from an array of current and pressure recording inverted echo sounders, and evidence of the recirculation gyres comes from profiling float data. Finally, they are also found in a high-resolution ocean general circulation model. Estimates of the transport in the jet and the recirculation gyres are made using the current meter data, the inverted echo sounders and numerical model.

2. Kuroshio Extension System Study

The Kuroshio Extension System Study (KESS) had its field program from June 2004 – June 2006 (Donohue et al. 2008). One of the goals of KESS is to understand the processes that govern the variability of and the interaction between the Kuroshio Extension and its recirculation gyres. The KESS field program observed a regime transition from a weakly meandering state to a strongly meandering state which occurred in late 2004. The weakly meandering pattern, which had begun in 2001, exhibited the characteristic pattern of two quasi-stationary meanders and a strong zonally-elongated southern recirculation gyre. Figure 1 displays the KESS observational array overlaid with the superposition of weekly snapshots of the Kuroshio's jet axis (here taken to be the 2.1 m sea surface height contour from the Aviso sea surface height product, similar to Qiu and Chen (2005)) giving the envelope of the jet's north-south meandering for the years 2004 – 2006. In December 2004 the Kuroshio Extension switched into its strongly meandering state in which its path became highly variable and eddy energy increased dramatically. The meandering spans several degrees of latitude, and during KESS, the jet crossed the axis of the mooring array as far south as the southern-most mooring (K-7), and as far north as the K-2 mooring (see Table 1

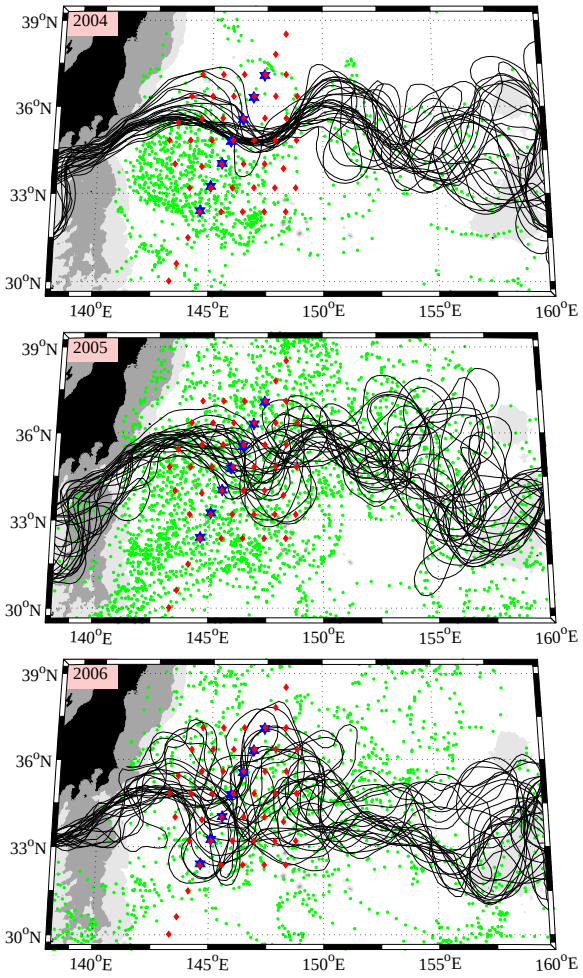

Figure 1. Geographical map of the KESS array. Overlaid are the positions of the current meter moorings (blue stars), CPIES (red diamonds) and Argo float locations (green dots). Black contour lines denote the 2.1 m contours of sea surface height at weekly intervals based on altimeter data for 2004, 2005 and 2006.

for locations).

Seven full-depth moorings with current meters, McLane moored profilers (MMP) and ADCPs were deployed for the 2-year period of the field program along a northeast-southwest tending line, coincident with a Jason satellite altimeter ground track (Figure 1). The array was centered on the first quasi-stationary meander trough of the Kuroshio Extension which also corresponds to the location of maximum time-average eddy kinetic energy (Qiu 2002). The current meter moorings were equipped with upward-looking ADCPs at 250 m housed in the moorings' subsurface spheres, MMPs which profiled between 250 m – 1500 m, and current meters at selected deeper depths. The current meters used were a mix of vector-averaging current meters (VACM) and Aanderaa RCM-11 acoustic current meters. They were deployed at 1500 m (VACM), 2000 m (RCM-11), 3500 m (RCM-11) and 5000 m (RCM-11). The RCM-11 current speeds were corrected for the speed of sound and adjusted upward by 10% to account for a bias in their measurement compared to other current meters (Hogg and Frye 2007). The current meters yielded almost complete time series at all sites (>80% data return), while the MMPs had problems. All the MMPs were working after deployments in 2004 and 2005, but typically stopped profiling in strong currents and the winter months. Despite these failures in high currents (50–100 cm s^{-1}), the MMPs returned temperature, salinity and velocity measurements at any given depth (250–1500 m) and any given day 55% of the time. Here we focus only on the observations from the current meters and leave the MMP data for a future analysis. Additionally the surface geostrophic velocity was estimated from the sea surface height observed from satellite altimetry.

Inverted echo sounders equipped with pressure sensors and current meters (CPIES) were deployed at 46 locations in an array surrounding the current meter moorings (Figures 1 and 5a). The CPIES array maps the velocity and density structure through the full water column (Donohue et al. 2009). The inverted echo sounder measures round-trip acoustic echo travel time of a 12.0 kHz pulse from sea bed to sea surface. Utilizing empirical relationships established with historical hydrography (the Gravest Empirical Mode (GEM) method, *e.g.* Meinen and Watts (2000); Sun and Watts (2001); Watts et al. (2001)), a look-up table between the echo travel time integrated from the surface to a chosen reference depth and hydrographic properties yields estimates of vertical profiles of temperature and density at each CPIES. Time-series profiles of geopotential thickness are estimated at each site, and through geostrophy, baroclinic shears are determined. Additionally, the measurements from the CPIES deep pressure gauges and current meters provide a reference velocity to make the baroclinic velocity profiles absolute. This method has been successfully used before in ocean jets (Meinen and Watts 2000; Book et al. 2002; Andres et al. 2008). The CPIES array had sufficient lateral spacing (nominally 88 km) to map mesoscale variability of the jet. The entire region was well observed for 16 months from June 2004 to September 2005 before some of the CPIES were lost to equipment failures. Donohue et al. (2009) provides a comprehensive discussion of CPIES processing techniques and associated instrumentation, GEM, and mapping errors from KESS. Briefly, pointwise root-mean-square differences between mapped and measured velocities were 15–20 cm s^{-1} near 200 m. These pointwise velocities include submesoscale and ageostrophic compo-

Mooring	Longitude Latitude	Comp.	Surface Altimetry	250 m ADCP	1500 m VACM	2000 m RCM-11	3500 m RCM-11	5000 m RCM-11
K-1	147.4°E	*u*	-9.4±28.0	-3.5±20.5	—	0.1±6.3	—	0.7±6.1
	37.1°N	*v*	-1.9±22.2	3.9±19.9	—	1.4±4.5	—	1.5±5.7
K-2	146.9°E	*u*	-2.5±29.6	-4.8±29.3	-1.7±7.4	-1.9±5.9	-1.2±6.2	-0.9±6.2
	36.3°N	*v*	-4.2±24.7	-13.3±28.7	0.3±6.5	0.3±4.9	0.7±5.2	1.5±5.3
K-3	146.4°E	*u*	38.1±38.4	18.5±35.1	-0.8±8.4	-2.0±7.0	-3.5±6.2	-3.7±6.4
	35.6°N	*v*	-29.0±53.5	-21.4±45.7	-1.4±8.5	-0.8±7.1	0.5±6.0	-0.4±5.7
K-4	146.1°E	*u*	58.8±58.3	30.9±45.0	1.1±8.4	1.2±7.3	-0.2±6.7	-0.4±6.9
	35.0°N	*v*	-33.7±49.5	-34.6±48.5	-2.2±7.6	-2.7±7.3	-0.8±6.2	-0.1±6.7
K-5	145.5°E	*u*	-2.4±48.0	15.1±41.5	1.8±7.7	0.9±6.0	1.1±6.3	1.6±7.3
	34.0°N	*v*	-14.7±50.6	-17.5±37.9	-3.8±7.5	-2.3±7.3	-1.4±7.6	-1.2±9.0
K-6	145.0°E	*u*	4.0±39.3	8.5±33.6	-2.2±5.9	-2.3±4.9	-2.5±5.1	-2.5±6.2
	33.3°N	*v*	2.6±50.9	-1.8±37.9	-2.0±7.5	-1.7±6.3	-1.4±6.2	-1.4±6.6
K-7	144.6°E	*u*	1.1±28.0	3.2±27.5	-1.8±5.8	-2.0±5.5	-1.6±4.5	-1.4±4.6
	32.4°N	*v*	5.4±17.6	1.5±21.6	-1.5±4.7	-1.6±4.1	-1.9±3.9	-3.0±4.4

Table 1. Time-average currents and their standard deviations calculated from the moored current meters. The surface currents are estimated from the AVISO sea surface height product assuming geostrophy. The currents at 250 m are taken from the ADCPs on the moorings. The currents at 1500 m were observed with vector-averaging current meters (VACM), and the currents at 2000 m, 3500 m and 5000 m where measured with Aanderaa RCM-11 current meters. The zonal velocity, u, and the meridional velocity, v, are positive to the east and north, and are in units of cm s^{-1}.

nents. Velocity errors decreased with depth and mapped errors were typically less than 6 cm s^{-1} (3 cm s^{-1}) near 500 m (800 m) depth. The error in the average near surface geostrophic velocity between adjacent CPIES is 10 cm s^{-1} (Donohue et al. 2009).

The KESS program also deployed 48 APEX profiling floats in the region of the Kuroshio Extension, which provided a detailed description of the temperature and salinity structures at 5 day intervals. Lagrangian velocities at their parking depth of 1500 m were computed from their displacements (Chen et al. 2007; Qiu et al. 2008). These observations are in addition to float displacements from the international Argo program which drifted at depths between 1000 m and 2000 m and generally profiled every 10 days (Lebedev et al. 2007). Together, these provide 4795 displacements in the region of 140–150°E and 32–37°N.

3. Observations

3.1. Current meters

Velocity timeseries: Figure 2 illustrates the raw timeseries of the zonal velocity from the current meters from two of the moorings, one to the north of time-average jet position (K-2) and one to the south of the time-average jet (K-6) (see Table 1 for locations). Additionally surface velocities were calculated at each mooring location from the sea surface height observed by altimetry assuming geostrophy. In the surface ocean, the strong currents associated with the meandering jet are observed. In the deep ocean, the current meter records reveal that the fluctuations are much smaller in magnitude than the surface ocean Furthermore the deep flow is uncorrelated with the surface flow, with vector correlations of in the range 0.1–0.3 between the surface velocity and abyssal velocities. However, amongst themselves the abyssal currents are highly vertically coherent (with vector correlations of greater than 0.8 between the three deepest current meters) and are largely barotropic in nature. The deep current meters at 1500 m show the largest variability since they are closest to the surface jet and the thermocline (comparing variances in Table 1 for 1500 m versus deeper levels). The current meters at 2000 m and 3500 m show relatively reduced variability, while those at 5000 m show a slight enhancement, compared to those at 3500 m. This enhancement of the variability near the bottom is likely the result of interactions of the currents with a sloping bottom (Salmon et al. 1976; Merryfield 1998).

The weak depth dependence of the velocity field is consistent with previous current meter observations from the Kuroshio Extension (Schmitz 1984; Schmitz et al. 1987). They found that the eddy field in the Kuroshio Extension is highly vertically coherent from the base of thermocline to 200 m above the ocean bottom from mooring observations located at 35°N, 152°E, which was slightly to the east of the

KESS array location. The KESS mooring observations similarly suggest that the abyssal ocean below the thermocline acts as a single layer (Waterman 2009).

Time-averaged velocity: The time-averaged velocity observations are tabulated in Table 1 along with their variances. It should be noted that the current's variance exceeds the mean at nearly every current meter because of the presence of a strongly meandering jet. Figure 3a shows these time-averaged velocity vectors of the mooring array in the upper ocean measured by the ADCP at 250 m on the moorings, and the surface velocity estimated from satellite altimetry, overlaid with the mean surface height contours from the time-averaged sea surface height from the KESS period (June 2004 – June 2006). The upper ocean velocity vectors show a strong surface-intensified jet as expected, and it is noted that the direct current measurements at 250 m and the geostrophic velocities estimated from altimetry assuming geostrophy agree well. Figure 3b shows the time-averaged velocity vectors in the deep ocean from current meters at 1500 m, 2000 m, 3500 m, and 5000 m. There is a strong indication of westward flow associated with recirculation gyres flanking the jet to the north and south.

The current meter array crosses the jet nearly perpendicular to a quasi-permanent meander in the jet. Because of the presence of this meander, a rotation of the velocity field into a coordinate system parallel and perpendicular to the array axis allows the core of the jet and the flanking flow to be more plainly seen than it would be in the zonal velocity component. Therefore we rotate the mean velocity vectors shown in Figure 3 by 26.2° to the right to get the cross-array velocity component and contour them as a function of latitude and depth (Figure 4a). We see a relatively wide ($\approx$ 250 km) jet in the upper ocean with an average velocity at the surface of about 68 cm s^{-1}. Again there is some evidence of westward flow on the north and south flanks of the jet.

A stream-coordinate time-average was constructed by locating the jet axis (defined by the 2.1 m sea surface height from the AVISO altimetry product which is the same contour plotted in Figure 1) relative to the array at each measurement time (see for example Halkin and Rossby 1985; Johns et al. 1995; Meinen et al. 2009; Howe et al. 2009). Then, at each mooring, the nearest point to the jet axis was located, and the distance to the mooring and the orientation to the jet axis at that point was computed. Using the orientation of the axis relative to the mooring array, the velocity components for each time were rotated into down-stream and cross-stream components. The distance between the moorings and jet axis were used to bin-average the down-stream and cross-stream velocities in time with a bin size of 25 km (about a quarter the spacing between the moorings, which was found to give reasonably smooth estimates). The stream-coordinate averaged, down-stream velocity component is shown in Figure 4b. In general more measurements make up the average near the jet axis compared to away from it as a result of the jet axis almost always being inside the array. The time-average in stream-coordinates represents a picture of the mean jet structure with the smearing effects of the jet meanders removed, and can be thought of as the mean synoptic jet. We see that the core of the jet is over twice as strong, with velocities of 152 cm s^{-1} in the stream-coordinate average versus 68 cm s^{-1} in the geographic average, the result of the core being smeared out by the meandering of the very strong jet. The stream-coordinate average also highlights the existence of weakly-depth dependent recirculations flanking the jet to both the north and the south that extend throughout the water column. Given the relatively weak magnitude of the recirculations relative to the baroclinic jet, we can see more clearly the westward flows of the recirculations that are absent in the geographical mean picture in the upper ocean. This is a consequence of occasional strong eastward velocities associated with the meandering jet dominating over the weak flanking flows and erasing them in the Eulerian time average (Hogg 1992).

3.2. CPIES

The CPIES array provides an mapped estimate of the absolute geostrophic flow for the period June 2004 through September 2005. Throughout the region, the mean currents turn with depth and tend to decrease in amplitude down to about 2000 m (Howe et al. 2009), as is also shown by the vectors in Figure 3. The time-averaged geopotential anomaly field at 1500 m is shown in Figure 5a. The currents at this level have substantial contributions from the abyssal and upper baroclinic flow, such that in the mean they closely resemble the vertically-integrated transport (Figure 5b), which will be discussed later. Along the path of the surface jet, a coherent, strong southeastward current exists at 1500 m along the north side of the southern recirculation (centered at 144°E, 24.3°N). To the north of the jet is a cyclonic circulation associated with the northern recirculation gyre (centered at 146.5°E, 35.5°N).

3.3. Floats

A total of 48 APEX profiling floats that were released as part of KESS were set to have a parking depth of 1500 (see Qiu and Chen 2005; Chen et al. 2007; Qiu et al. 2008, for more details). Additional Argo floats with parking depths of 1000 m, 1500 m, and 2000 m were taken from the YoMaHa'07 database (Lebedev et al. 2007). To correct the additional Argo float displacements to a uniform depth, their drifts were corrected for the time-average shear to estimate the Lagrangian velocities at 1500 m. The resulting displace-

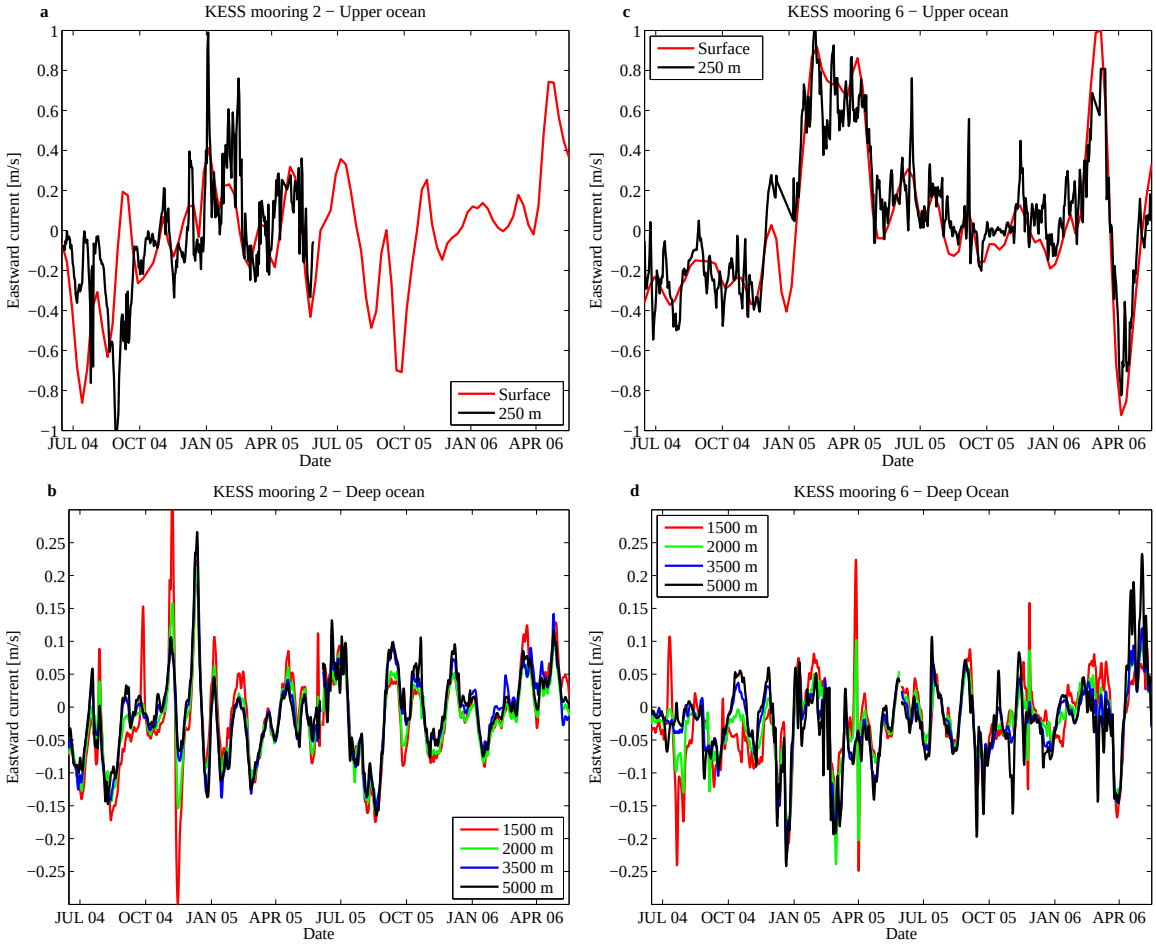

Figure 2. The timeseries of the zonal velocity at the K-2 mooring in the upper ocean (a) and the lower left in the deep ocean (c). The timeseries of the zonal velocity at the K-6 mooring in the upper ocean (b) and the in the deep ocean (d). Note the change in scale between the upper and deep ocean plots. The velocity at the surface was calculated from altimetry assuming geostrophy.

ments were then bin-averaged in to nominal 1° bins to calculate the Eulerian space-time average velocities and their statistical uncertainties (Davis 1998; Lavender et al. 2005). The bin-averaged velocities and sampling errors were then mapped by objective analysis using the technique of Bretherton et al. (1976) assuming a non-divergent velocity field and a length scale of 100 km to estimate the geostrophic pressure field at 1500 m (Figure 6). The mapped geostrophic pressure field is that which would be associated with the flow field presented by Qiu et al. (2008, see their figure 4). The same general features that are seen in the pressure map from the CPIES (Figure 5a) can be seen here, but with a wider geographic coverage. The profiling float drifting data reveals that the northern recirculation gyre extends from 144°E east of Japan all the way to about 159°E, where it is blocked by the meridionally-aligned Shatsky Rise.

4. Numerical model results

The ocean general circulation model simulation utilized for this study is an eddying run of the Parallel Ocean Program (POP, see Smith et al. 1992; Maltrud and McClean 2005; McClean et al. 2006, 2008). POP is a three-dimensional, z-level, primitive equation model. For this simulation it was configured on a 40-vertical level, 1/10° global grid, with the numerical grid's North Pole displaced into Hudson Bay. In the region of the Kuroshio Extension, the model has a local resolution of 9 km in zonal direction, and 11 km in the meridional direction. The model was initialized

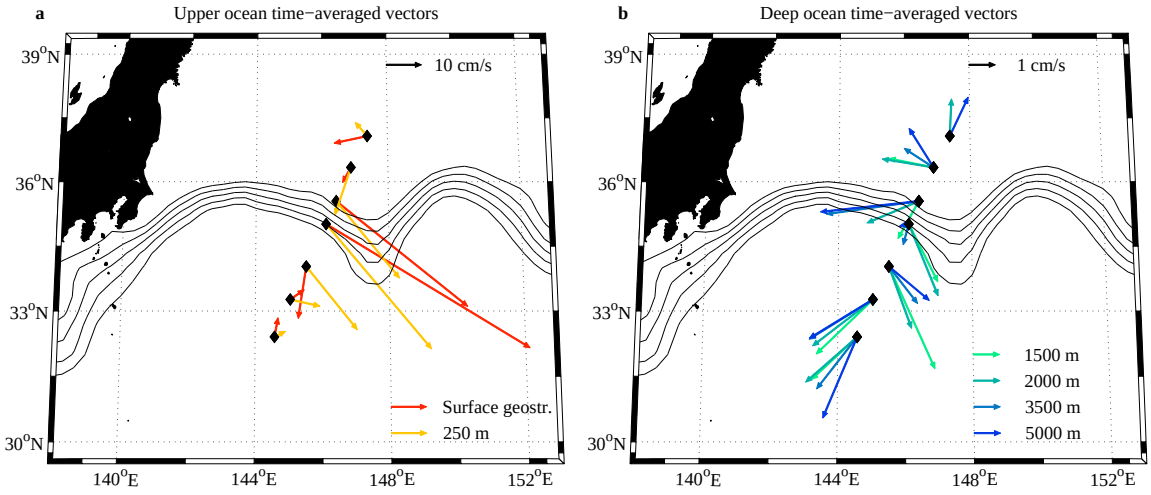

Figure 3. Time-averaged velocity vectors form the moored current meters: (a) the upper ocean (surface and 250 m), and (b) the deep ocean (1500 m, 2000 m, 3500 m, and 5000 m). Overlaid are the positions of the 1.9–2.3 m contours of time-average sea surface height from AVISO for the KESS period. The velocity at the surface was calculated from altimetry assuming geostrophy. Note the change in the scaling of the vectors between the two panels.

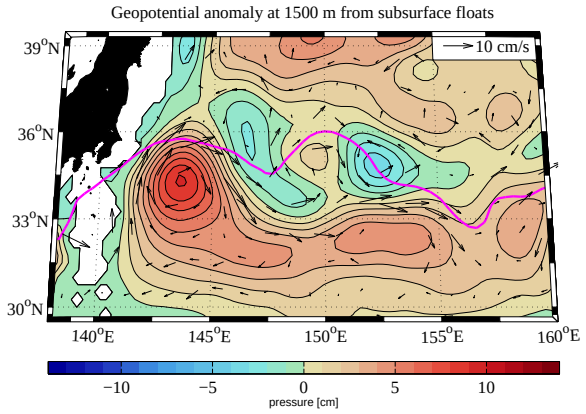

Figure 6. Time-averaged geopotential anomaly at 1500 m objectively mapped from profiling float displacements for the KESS period. The units are dynamic centimeters. The KESS-period time-averaged position of the 2.1 m sea surface height contour (from Aviso) is over-plotted to indicate the location of the surface jet.

from the Navy's Modular Ocean Data Assimilation System (MODAS) climatology (Fox et al. 2002), except in the Arctic Ocean where the Polar Hydrographic Climatology was used (Steele et al. 2001). No data assimilation was used in the model simulation. The model was forced with synoptic atmospheric fluxes derived from the NCEP-NCAR reanalysis product (Large and Yeager 2004) for the period from 1979–2003. This simulation was previously used to examine the formation and variability of the North Pacific Subtropical Mode water in the KESS region for a three year period (1998–2000) by Rainville et al. (2007), and additional model-data intercomparisons can be found therein. Here we utilize the same three year period to examine the model's recirculation gyres.

It should be noted that a deficiency of the model simulation is that over the 3-year period which is available, there was no regime shift from a weakly-meandering state to a strongly-meandering state as the model stayed in the weakly-meandering state for the whole 3 years. This has the effect of highlighting the recirculation gyres since during the strongly-meandering state of the Kuroshio Extension the westward flow associated with the recirculation gyres tend to get smeared out by the time averaging.

In order to more easily visualize the abyssal circulation, the geostrophic geopotential anomalies at 1500 m and 5000 m, and depth-integrated transport streamfunction was computed as follows. Using the same methodology as was applied to the float data, the daily velocity fields from the model simulation were binned into 0.5° bins, then objectively mapped to derive the total transport streamfunction and geostrophic geopotential anomaly at the selected depths, and finally averaged in time. The surface height field and geopotential anomalies at 1500 m and 5000 m are shown in Figures 7b and 7c. What is notable is that there are elon-

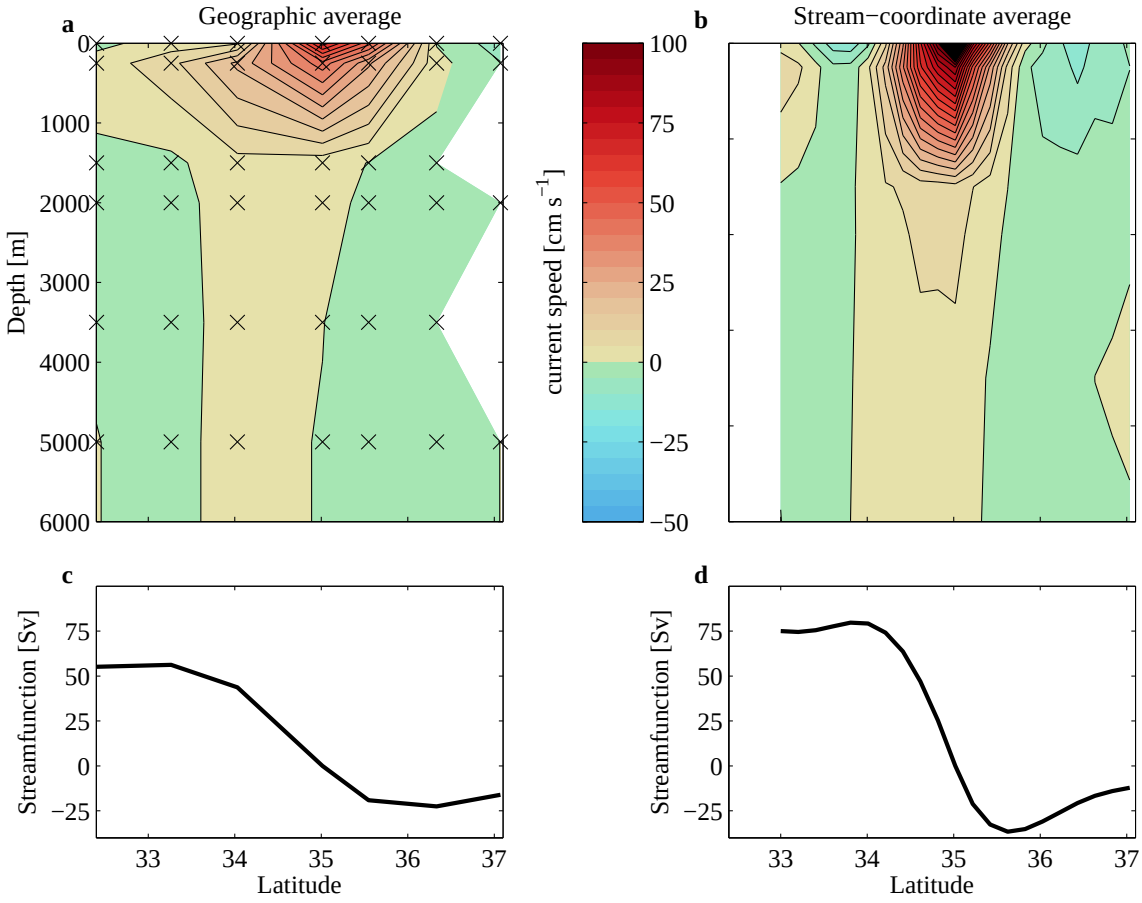

Figure 4. Contours of time-averaged velocity perpendicular to the mooring array averaged in (a) geographic coordinates with black '×'s indicating the locations of current meters and (b) the time-averaged down-stream velocities averaged in stream coordinates. The time-average center of the stream-coordinate system was at approximately 35°N. Panels (c) and (d) show the vertically integrated transport streamfunction in Sverdrups.

gated recirculation gyres to the north and south of the jet which are modulated in amplitude by the meander crests and troughs. The overall recirculation fields extend about 1000 km in the meridional direction, but they are concentrated into several cells of order 400 km in lengthscale. This is quite different than the recirculation in the Gulf Stream, where single elongated flanking gyres with lengthscales on the order of 2000 km along-jet and 500 km cross-jet flank the Gulf Stream (Hogg 1992). The surface pressure field shows almost no signature of this circulation, similar to the findings of Nakano et al. (2008). Additionally, as in Nakano et al. (2008), the deeper pressure fields in the model show multiple closed contours to both the north and south of the jet, supporting the KESS observations of a time-averaged recirculation gyres to the north and south of the jet.

5. Transport estimates

Imawaki et al. (2001) estimated that Kuroshio at Cape Ashizuri on the south coast of Japan (located about 133°E) carries 42±1.6 Sv (averaged over the time period from 1992-1999), excluding the contribution from the local recirculations. This transport estimate was made from the combination of hydrographic surveys and current meter moorings maintained along the Affiliated Surveys of the Kuroshio off Cape Ashizuri (ASUKA) observation line. The transport across the ASUKA line was correlated with sea surface height measured by satellite altimetry along the line to establish a means of long-term monitoring the Kuroshio transport that continues through the present. During the KESS period the average transport was 45±11 Sv, slightly higher than the long term average (data from the ASUKA website:

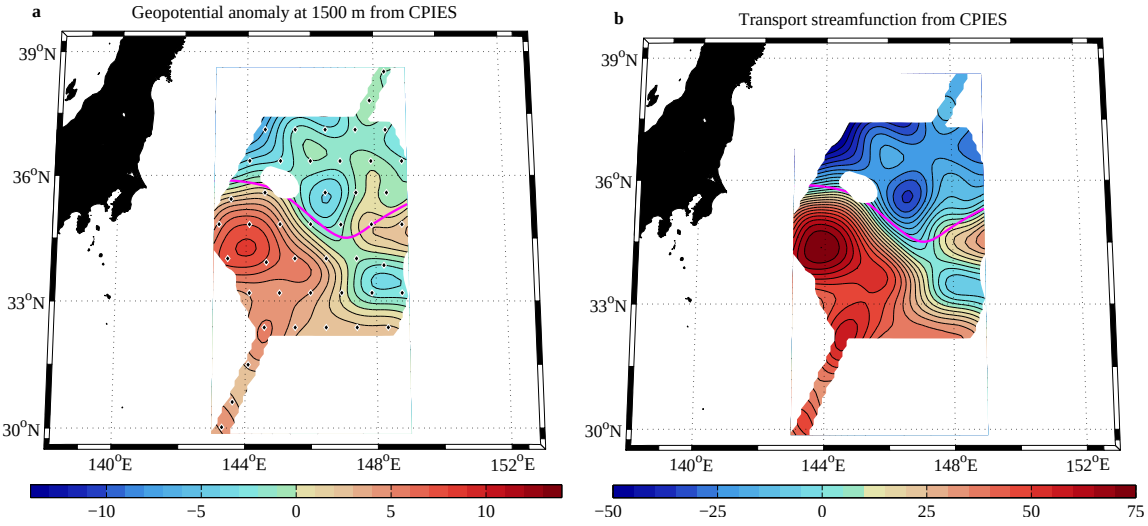

Figure 5. (a) Time-averaged geopotential anomaly (in dynamic centimeters) at 1500 m mapped with the CPIES array over the period June 2004–September 2005. The locations of the CPIES used in the mapping are shown by black dots. The mean location of the upper Kuroshio Extension jet, also derived from the CPIES measurements for the same 16-month period, is superimposed. (b) The time-averaged transport streamfunction (in Sverdrups) vertically-integrated between the surface and 5300 m for the same 16-month period.

http://www.riam.kyushu-u.ac.jp/oed/asuka/alt/index.html). This transport estimate provides a reference from which to quantify the enhancement of the transport in the Kuroshio Extension after it separates from the coasts and develops recirculation gyres.

The current meter data from the KESS array can be used to estimate the total downstream transport of the combined Kuroshio Extension and its recirculation gyres across the array. Taking the depth integral of the stream-coordinate time-averaged current meter velocity and then performing a second integration in the cross-stream direction yields an estimate of the transport streamfunction across the current meter array. A total downstream transport of 114±13Sv across the KESS current mooring array is estimated (Figure 4b), with the error estimate taking into account temporal variability (the dominant source of uncertainty), binning error, and uncertainty in the depth. A similar transport can be estimated from the simple time-averages at each mooring (*i.e.* the Eulerian average), which gives a weaker estimate of 79 Sv for the total transport (Figure 4a). This reduction of 31% in the jet and recirculation strength of the Kuroshio Extension in the Eulerian averaging compared to the stream-coordinate average is very similar to the 38% reduction seen in the Eulerian average of the Gulf Stream of 93 Sv (Richardson 1985) compared to 150 Sv in the stream-coordinate average (Hogg 1992). Estimates of the transport during the weakly-meandering state and the strongly-meandering state are quite similar, 109 Sv and 119 Sv respectively (Table 2).

The transport estimate from the CPIES, calculated between the center of the southern recirculation gyre to the center of the northern recirculation gyre, represents a geographic average (not the stream-coordinate average) and is made over a slightly different time period, is of similar magnitude at 111 Sv (Figure 5). Transports between the southern and the northern recirculation gyres estimated separately for the two periods from CPIES array show higher transports during the weakly-meandering state (155 Sv) than the strongly-meandering state (93 Sv) (see Table 2). Howe et al. (2009) estimate a transport of 124 Sv at the same location as the mooring array based on a stream-coordinate analysis of the CPIES data averaged over the first 5.5 months (1 June – 16 November 2004), with a higher transport of 138 Sv upstream at 143°E at the first quasi-stationary crest of the Kuroshio Extension, and a lower transport of 75 Sv entering the second crest.

By comparison, there are a few prior estimates of the Kuroshio Extension transport. Farther downstream the KESS array, a historical estimate was made by Hall (1989), who calculated a transport of 87±21 Sv from a single mooring located at 152°E. More recently, from a synoptic section using lowered ADCP Yoshikawa et al. (2004) calculated a transport of 113 Sv across 152.5°E. They also suggest that the Hall (1989) estimate missed about 10 Sv of eastward flow on the southside of the current, and hence her estimate should

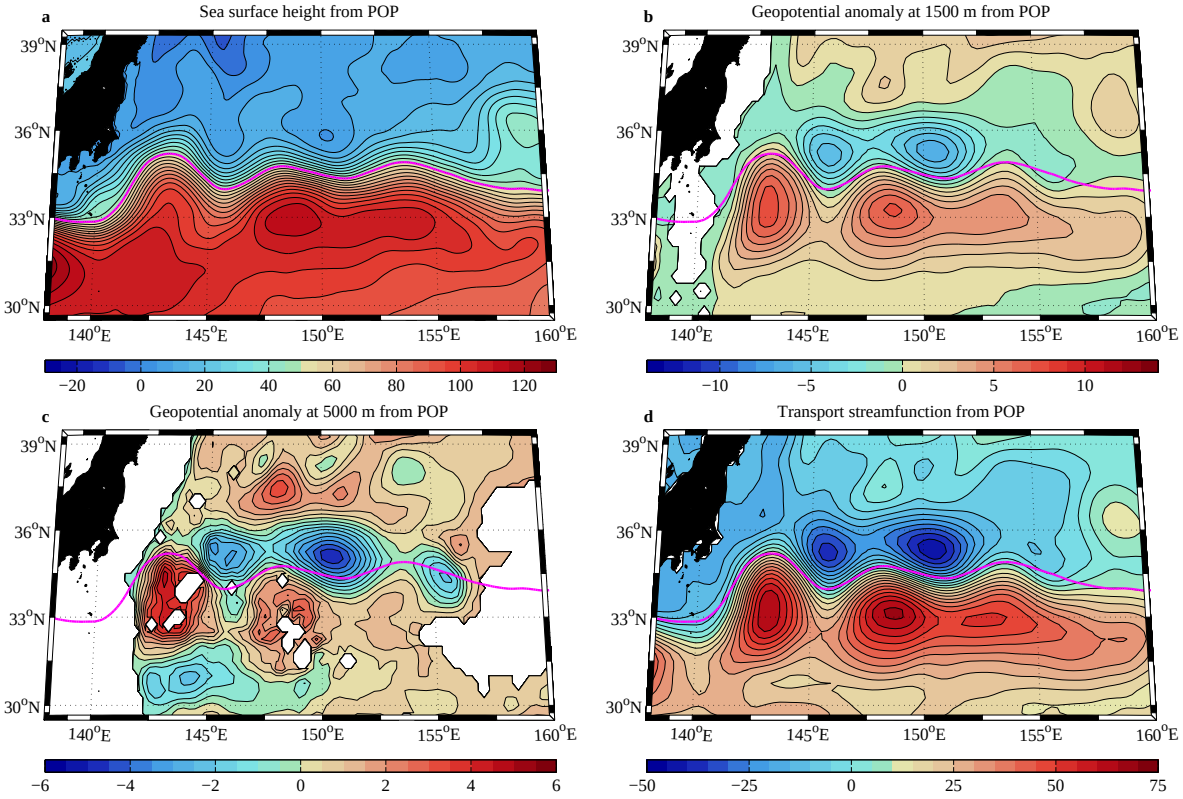

Figure 7. Time-averaged sea surface height (a), geopotential anomaly at 1500 m (b) and 5000 m (c), and the depth-integrated transport streamfunction (d) from POP model. The units on the sea surface height are centimeters, the geopotential is in dynamic centimeters, and the transport streamfunction is in Sverdrups. The time-averaged 0.5 m sea surface height contour from the model is over-plotted to indicated the location of the surface jet.

Method	Averaging	Time period	Location	Transport [Sv]
Current meters	Stream-coordinate	6/2004–6/2006	KESS mooring line	114
Current meters	Stream-coordinate	6/2004–11/2004	KESS mooring line	109
Current meters	Stream-coordinate	12/2004–6/2006	KESS mooring line	119
Current meters	Geographic	6/2004–6/2006	KESS mooring line	79
CPIES ¶	Stream-coordinate	6/2004–11/2004	across first trough	124
CPIES	Geographic	6/2004–9/2005	between SRG and NRG	111
CPIES	Geographic	6/2004–11/2004	between SRG and NRG	155
CPIES	Geographic	12/2004–9/2005	between SRG and NRG	93
POP model	Geographic	1998–2000	between SRG and NRG	102

Table 2. Transport estimates of the Kuroshio Extension and its recirculation gyres from the KESS observations and POP model. Included is a transport estimate from ¶ Howe et al. (2009). The time period from 16 June 2004 through 16 November 2004 corresponds to when the jet was in its weakly-meandering state, while the period from 17 November 2004 – 19 May 2006 the jet is strongly meandering. The transports calculated from the CPIES and POP model using the geographic averages are between the center of the southern recirculation gyre (SRG) to the center of the northern recirculation gyre (NRG).

be about 97 Sv. More relevant to the KESS observations presented here, is their estimate of 163 Sv across 146.4°E. In the same region, separate estimates of the transport in the southern recirculation gyre were 86 Sv observed by Firing (1998) using a lowered ADCP during WOCE on the P10 line (see also Wijffels et al. 1998), and 101 Sv estimated by Chen et al. (2007) from subsurface floats during KESS.

The larger scale picture provided by the POP model (Figure 7b) shows that there are a series of recirculation gyres to the north and south of the jet, located under the crests and above the troughs. This demonstrates the difficulties of trying to observe the transport in the Kuroshio Extension, and may explain the wide range of transport estimates, as such observations, even in the time average, will be very sensitive to the exact location of the measurement system. The meandering of the jet and the presence of detached rings further complicates the picture.

In the POP simulation (Figure 7d), the transport increases from 41 Sv carried by the jet at Cape Ashizuri (notably within the error bounds on the ASUKA estimate) to 102 Sv across the first permanent meander trough (near where the KESS array was) between the first set of southern and northern recirculation gyres, and 110 Sv across the second permanent meander trough between the second set of southern and northern recirculation gyres. At 152°E, the longitude of the WESTPAC array (Schmitz et al. 1987), the Hall (1989) analysis, and one of sections from Yoshikawa et al. (2004), the POP simulation has a mean total transport of 75 Sv. However, it should be noted that this longitude cuts through the eastern edge of the recirculation gyre system (Figure 7d) in the model and therefore the transport estimate there will be highly sensitive to the zonal extent of recirculation gyres which varies in time. Also, from the POP simulation it can be seen that the southern recirculation gyre (maxima of 64 Sv for the first cell at 143°E and 66 Sv for the second at 149°E) is stronger at than the northern recirculation gyre (minima of -37 Sv for the first cell at 146°E and -44 Sv for the second at 150°E). On the whole the high-resolution POP simulation appears to reproduce the Kuroshio Extension system reasonably well. It is important that models correctly represent these recirculation gyres as the realistic depiction of these features is critical for fidelity in air-sea interactions in western boundary current extension regions, and the models can ultimately provide insight into the recirculation gyre's dynamics.

6. Summary and Discussion

The combination of observations from the KESS program, in addition to a high-resolution numerical model, support the presence of quasi-permanent recirculation gyres to the north and south of the Kuroshio Extension jet. While the recirculation gyre to the south of the jet has been previously observed (Qiu et al. 1991; Wijffels et al. 1998; Niiler et al. 2003a; Yoshikawa et al. 2004; Qiu and Chen 2005; Chen et al. 2007; Qiu et al. 2008) the northern recirculation gyre is first clearly identified in the KESS observations (see also Qiu et al. 2008). The recirculation gyres appear to significantly enhance the local circulation by increasing the transport of the Kuroshio from 42 Sv when it separates from the coast (Imawaki et al. 2001) to 114 Sv at the KESS array (a increase of about 2.7 times).

The numerical model results show series of recirculation cells flanking the jet. Furthermore, the model results show that the southern recirculation gyre appears to be much stronger and the northern gyre correspondingly weaker. The modulation of the overall recirculation gyres in the Kuroshio Extension by the crests and troughs appear to be quite different from those in the Gulf Stream where elongated gyres of almost equal strength are found flanking the stream (Hogg 1992). The north-south asymmetry in the transport of the recirculation gyres is likely due to the presence of quasi-stationary meanders in the mean path of the Kuroshio Extension.

Previous studies on the Kuroshio Extension's quasi-stationary meanders have argued about the dynamics of the meanders. In particular White and McCreary (1976) argue that the quasi-stationary meanders are the outcome of standing Rossby waves, while others find that they are maintained by the convergence of the eddy potential vorticity flux (Hurlburt et al. 1996; Qiu and Chen 2009). It is difficult to know at present how the recirculation gyres fit into this dynamical picture. Qiu et al. (2008) find that the northern recirculation gyre is driven by radiating eddy fluxes. Future work should seek to elucidate the dynamical connection between the quasi-permanent meanders, the recirculation gyres, and eddy fluxes.

Acknowledgments.

This work was supported by National Science Foundation funding for the KESS program under grants OCE-0220161 (SRJ, NGH, LR and SNW), OCE-0825550 (SNW), OCE-0221008 (KAD, DRW, KLT), OCE-0220680 (BQ, SC and PH), and OCE-0549225 (JLM). We would like to thank the ships' crews of the *R/V Thompson*, *R/V Revelle*, and *R/V Melville*, and the WHOI Subsurface Mooring Operations Group for their assistance in the KESS field program. More information and the observational data from KESS can be found at: *http://uskess.org*.

References

Andres, M., M. Wimbush, J.-H. Park, K.-I. Chang, B.-H. Lim, D. R. Watts, H. Ichikawa, and W. J. Teague, 2008: Observations

of Kuroshio flow variations in the East China Sea. *J. Geophys. Res.*, **113**, C05013, doi:10.1029/2007JC004200.

Beal, L. M., J. M. Hummon, E. Williams, O. B. Brown, W. Baringer, and E. J. Kearns, 2008: Five years of Florida Current structure and transport from the Royal Caribbean Cruise ship *Explorer of the Seas*. *J. Geophys. Res.*, **113**, C06001, doi:10.1029/2007JC004154.

Beliakova, N. Y., 1998: *Generation and Maintenance of Recirculations by Gulf Stream Instabilities*. Ph.D. thesis, Mass. Inst. of Technol./Woods Hole Oceanogr. Inst. Joint Program, Cambridge, MA.

Berloff, P., 2005: On the rectification of randomly forced flows. *J. Mar. Res.*, **63**, 497–527.

Book, J., M. Wimbush, S. Imawaki, H. Ichikawa, H. Uchida, and H. Kinoshita, 2002: Kuroshio temporal and spatial variations south of Japan determined from inverted echo sounder measurements. *J. Geophys. Res.*, **107**, C3121, doi:10.1029/2001JC000795.

Bretherton, F. P., R. Davis, and C. Fandry, 1976: A technique for objective analysis and design of oceanographic experiments. *Deep-Sea Res.*, **23**, 559–582.

Cessi, P., 1990: Recirculation and separation of boundary currents. *J. Mar. Res.*, **48**, 1–35.

Cessi, P., G. Ierley, and W. Young, 1987: A model of the inertial recirculation driven by potential vorticity anomalies. *J. Phys. Oceanogr.*, **17**, 1640–1652.

Chen, S., B. Qiu, and P. Hacker, 2007: Profiling float measurements of the recirculation gyre south of the Kuroshio Extension in May to November 2004. *J. Geophys. Res.*, **112**, C05023, doi:10.1029/2006JC004005.

Cronin, M., 1996: Eddy-mean flow interaction in the Gulf Stream at 68°W. Part II: Eddy forcing on the time-mean flow. *J. Phys. Oceanogr.*, **26**, 2132–2151.

Cronin, M., and D. R. Watts, 1996: Eddy-mean flow interaction in the Gulf Stream at 68°W. Part I: Eddy energetics. *J. Phys. Oceanogr.*, **26**, 2107–2131.

Davis, R. E., 1998: Preliminary results from directly measuring middepth circulation in the tropical and South Pacific. *J. Geophys. Res.*, **103**, 24,619–24,639.

Donohue, K. A., D. R. Watts, K. L. Tracey, A. D. Greene, and M. Kennelly, 2009: Mapping circulation in the Kuroshio Extension with an array of current and pressure recording inverted echo sounder. *J. Atmos. Oceanic Technol.*, in press.

Donohue, K. A., D. R. Watts, K. Trcaey, M. Wimbush, J.-H. Park, N. Bond, M. Cronin, S. Chen, B. Qiu, P. Hacker, N. Hogg, S. Jayne, J. McClean, L. Rainville, H. Mitsudera, Y. Tanimoto, and S.-P. Xie, 2008: Program studies the Kuroshio Extension. *EOS Trans. Amer. Geophys. Union*, **89**, 161–162.

Firing, E., 1998: Lowered ADCP development and use in WOCE. *International WOCE Newsletter*, **30**, 10–14.

Fofonoff, N. P., 1954: Steady flow in a frictionless homogeneous ocean. *J. Mar. Res.*, **50**, 545–566.

Fox, D., W. Teague, C. Barron, M. Carnes, and C. Lee, 2002: The modular ocean data assimilation system (MODAS). *J. Atmos. Oceanic Technol.*, **19**, 240–252.

Greatbatch, R. J., 1987: A model for the inertial recirculation of a gyre. *J. Mar. Res.*, **45**, 601–634.

Haidvogel, D. B., and P. B. Rhines, 1983: Waves and circulation driven by oscillatory winds in an idealized ocean basin. *Geophys. Astrophys. Fluid Dyn.*, **25**, 1–63.

Halkin, D., and T. Rossby, 1985: The structure and transport of the Gulf Stream at 73°W. *J. Phys. Oceanogr.*, **15**, 1439–1452.

Hall, M. M., 1989: Velocity and transport structure of the Kuroshio Extension at 35°N, 152°E. *J. Geophys. Res.*, **94**, 14,445–14,459.

Hogg, N. G., 1983: A note on the deep circulation of the western North Atlantic: Its nature and causes. *Deep-Sea Res.*, **30**, 945–961.

Hogg, N. G., 1985: Evidence for baroclinic instability in the Gulf Stream recirculation. *Prog. Oceanog.*, **14**, 209–229.

Hogg, N. G., 1992: On the transport of the Gulf Stream between Cape Hatteras and the Grand Banks. *Deep-Sea Res.*, **39**, 1231–1246.

Hogg, N. G., 1993: Toward parameterization of the eddy field near the Gulf Stream. *Deep-Sea Res.*, **40**, 2359–2376.

Hogg, N. G., and D. E. Frye, 2007: Performance of a new generation of acoustic current meters. *J. Phys. Oceanogr.*, **37**, 148–161.

Hogg, N. G., and W. E. Johns, 1995: Western boundary currents. U.S. National Report to the IUGG. *Rev. Geophys.*, **33** (Suppl.), 1311–1334.

Hogg, N. G., R. S. Pickart, R. M. Hendry, and W. J. Smethie Jr., 1986: The northern recirculation gyre of the Gulf Stream. *Deep-Sea Res.*, **33**, 1139–1165.

Howe, P. J., K. A. Donohue, and D. R. Watts, 2009: Stream-coordinate structure and variability of the Kuroshio Extension. *Deep-Sea Res. I*, in press.

Hurlburt, H. E., A. J. Wallcraft, W. J. Schmitz, Jr., P. J. Hogan, and E. J. Metzger, 1996: Dynamics of the Kuroshio/Oyashio current system using eddy-resolving models of the North Pacific Ocean. *J. Geophys. Res.*, **101**, 941–976.

Imawaki, S., H. Uchida, H. Ichikawa, M. Fukasawa, S. Umatani, and ASUKA Group, 2001: Satellite altimeter monitoring the Kuroshio transport south of Japan. *Geophys. Res. Lett.*, **28**, 17–20.

Jayne, S. R., and N. G. Hogg, 1999: On recirculation formed by an unstable jet. *J. Phys. Oceanogr.*, **29**, 2711–2718.

Jayne, S. R., N. G. Hogg, and P. Malanotte-Rizzoli, 1996: Recirculation gyres forced by a beta-plane jet. *J. Phys. Oceanogr.*, **26**, 492–504.

Johns, W. E., T. J. Shay, J. M. Bane, and D. R. Watts, 1995: Gulf stream structure, transport, and recirculation near 68°. *J. Geophys. Res.*, **100**, 817–838.

Kawai, H., 1972: Hydrography of the Kuroshio Extension. in H. Stommel and K. Yoshida, editors, *Kuroshio — Its Physical Aspects*, pp. 235–354. University of Tokyo Press.

Large, W., and S. Yeager, 2004: Diurnal to decadal global forcing for ocean and sea-ice models: the data sets and flux climatologies. Tech. Rep. NCAR/TN-460+STR, National Center for Atmospheric Research.

Lavender, K. L., W. B. Owens, and R. E. Davis, 2005: The mid-depth circulation of the subpolar North Atlantic Ocean as measured by subsurface floats. *Deep-Sea Res.*, **52**, 767–785.

Lebedev, K. V., H. Yoshinari, N. A. Maximenko, and P. W. Hacker, 2007: YoMaHa'07: Velocity data assessed from trajectories of Argo floats at parking level and at the sea surface. Tech. Rep. 4(2), Int. Pac. Res. Cent., Univ. of Hawaii at Manoa, Honolulu, Hawaii.

Malanotte-Rizzoli, P., N. G. Hogg, and R. E. Young, 1995: Stochastic wave radiation by the Gulf Stream: Numerical experiments. *Deep-Sea Res.*, **42**, 389–423.

Maltrud, M. E., and J. L. McClean, 2005: An eddy resolving global 1/10° ocean simulation. *Ocean Modelling*, **8**, 31–54.

Marshall, J., and G. Nurser, 1986: Steady, free circulation in a stratified quasi-geostrophic ocean. *J. Phys. Oceanogr.*, **16**, 1799–1813.

McClean, J. L., S. R. Jayne, M. E. Maltrud, and D. P. Ivanova, 2008: The fidelity of ocean models with explicit eddies. in M. W. Hecht and H. Hasumi, editors, *Ocean Modeling in a Eddying Regime*, Vol. 177, pp. 149–163. AGU Monograph Series.

McClean, J. L., M. E. Maltrud, and F. O. Bryan, 2006: Measures of the fidelity of eddying ocean models. *Oceanography*, **19**, 104–117.

Meinen, C. S., D. S. Luther, and M. O. Baringer, 2009: Structure, transport and potential vorticity of the gulf stream at 68°W: Revisiting older data sets with new techniques. *Deep-Sea Res. I*, **56**, 41–60.

Meinen, C. S., and D. R. Watts, 2000: Vertical structure and transport on a transect across the North Atlantic Current near 42°N: Timeseries and mean. *J. Geophys. Res.*, **105**, 21,869–21,891.

Merryfield, W. J., 1998: Effects of stratification on quasi-geostrophic inviscid equilibria. *J. Fluid Mech.*, **354**, 345–356.

Mizuno, K., and W. B. White, 1983: Annual and interannual variability in the Kuroshio Current system. *J. Phys. Oceanogr.*, **13**, 1847–1867.

Mizuta, G., 2009: Rossby wave radiation from an eastward jet and its recirculations. *J. Mar. Res.*, in press.

Nakano, H., H. Tsujino, and R. Furue, 2008: The Kuroshio current system as a jet and twin "relative" recirculation gyres embedded in the Sverdrup circulation. *Dyn. Atmos. Oceans*, **45**, 135–164.

Niiler, P. P., N. A. Maximenko, and J. C. McWilliams, 2003a: Dynamically balanced absolute sea level of the global ocean derived from near-surface velocity observations. *Geophys. Res. Lett.*, **30**, 2164, doi:10.1029/2003GL018628.

Niiler, P. P., N. A. Maximenko, G. G. Panteleev, T. Yamagata, and D. B. Olson, 2003b: Near-surface dynamical structure of the Kuroshio Extension. *J. Geophys. Res.*, **108**, 3193, doi:10.1029/2002JC001461.

Owens, W. B., and B. A. Warren, 2001: Deep circulation in the northwest corner of the Pacific Ocean. *Deep-Sea Res. I*, **48**, 959–993.

Qiu, B., 2002: The Kursohio Extension System: Its large-scale variability and role in the midlatitude ocean-atmosphere interaction. *J. Oceangr.*, **58**, 57–75.

Qiu, B., and S. Chen, 2005: Variability of the Kuroshio Extension jet, recirculation gyre and mesoscale eddies on decadal timescales. *J. Phys. Oceanogr.*, **35**, 2090–2103.

Qiu, B., and S. Chen, 2009: Eddy-mean flow interaction in the decadally-modulating Kuroshio Extension system. *Deep-Sea Res. II*, in press.

Qiu, B., S. Chen, P. Hacker, N. G. Hogg, S. R. Jayne, and H. Sasaki, 2008: The Kuroshio Extension northern recirculation gyre: Profiling float measurements and forcing mechanism. *J. Phys. Oceanogr.*, **38**, 1764–1779.

Qiu, B., K. A. Kelly, and T. M. Joyce, 1991: Mean flow and variability in the Kuroshio Extension from Geosat altimetry data. *J. Geophys. Res.*, **96**, 18,491–18,507.

Rainville, L., S. R. Jayne, J. L. McClean, and M. E. Maltrud, 2007: Formation of subtropical mode water in a high-resolution POP simulation of the Kuroshio Extension region. *Ocean Modelling*, **17**, 338–356.

Richardson, P. L., 1985: Average velocity and transport of the Gulf Stream near 55°W. *J. Mar. Res.*, **43**, 83–111.

Salmon, R., G. Holloway, and M. C. Hendershott, 1976: The equilibrium statistical mechanics of simple quasi-geostrophic models. *J. Fluid Mech.*, **75**, 691–703.

Schmitz, Jr., W. J., 1984: Observations of the vertical structure of the eddy field in the Kuroshio Extension. *J. Geophys. Res.*, **89**, 6355–6364.

Schmitz, Jr., W. J., and M. S. McCartney, 1993: On the North Atlantic circulation. *Rev. Geophys.*, **31**, 29–49.

Schmitz, Jr., W. J., P. P. Niiler, and C. J. Koblinsky, 1987: Two-year moored instrument results along 152° E. *J. Geophys. Res.*, **92**, 10,826–10,834.

Smith, R. D., J. K. Dukowicz, and R. C. Malone, 1992: Parallel ocean general circulation modeling. *Physica D.*, **60**, 38–61, doi:10.1016/0167–2789(92)90225–C.

Spall, M. A., 1994: Wave-induced abyssal recirculations. *J. Mar. Res.*, **52**, 1051–1080.

Steele, M., R. Morley, and W. Ermold, 2001: PHC: A global ocean hydrography with a high-quality Arctic Ocean. *J. Climate*, **14**, 2079–2087.

Sun, C., and D. R. Watts, 2001: A circumpolar gravest empirical mode for Southern Ocean hydrography. *J. Geophys. Res.*, **106**, 2833–2855.

Teague, W. J., M. J. Carron, and P. J. Hogan, 1990: A comparison between the Generalized Digital Environmental Model and Levitus climatologies. *J. Geophys. Res.*, **95**, 7167–7183.

Waterman, S., 2009: *Eddy-mean flow interactions in western boundary current jets*. Ph.D. thesis, Mass. Inst. of Technol./Woods Hole Oceanogr. Inst. Joint Program, Cambridge, MA.

Watts, D. R., X. Qian, and K. L. Tracey, 2001: Mapping abyssal current and pressure fields under the meandering Gulf Stream. *J. Atmos. Oceanic Technol.*, **18**, 1052–1067.

White, W. B., and J. P. McCreary, 1976: On the formation of the Kuroshio meander and its relationship to the large-scale ocean circulation. *Deep-Sea Res.*, **23**, 33–47.

Wijffels, S., M. Hall, T. Joyce, D. J. Torres, P. Hacker, and E. Firing, 1998: Multiple gyres of the western North Pacific: A WOCE section along 149°E. *J. Geophys. Res.*, **103**, 12,985–13,009.

Worthington, L. V., 1976: On the North Atlantic Circulation. The Johns Hopkins Oceanographic Studies, Vol. 6, 110 pp.

Yasuda, I., 2003: Hydrographic structure and variability in the Kuroshio-Oyashio transition area. *J. Oceangr.*, **59**, 389–402.

Yoshikawa, Y., J. A. Church, H. Uchida, and N. J. White, 2004: Near bottom currents and their relation to the transport in the Kuroshio Extension. *Geophys. Res. Lett.*, **31**, L16309, doi:10.1029/2004GL020068.

S. R. Jayne, Department of Physical Oceanography, Woods Hole Oceanographic Institution, MS 21, 360 Woods Hole Road, Woods Hole, MA 02543-1541. (e-mail: surje@alum.mit.edu)

Received July 1, 2009